PHYSICAL REVIEW C **66**, 041602(R) (2002)

Fusion and breakup in the reactions of ^{6}Li and ^{7}Li nuclei with ^{209}Bi

M. Dasgupta,[1] D. J. Hinde,[1] K. Hagino,[2] S. B. Moraes,[3] P. R. S. Gomes,[3] R. M. Anjos,[3] R. D. Butt,[1] A. C. Berriman,[1] N. Carlin,[4] C. R. Morton,[1] J. O. Newton,[1] and A. Szanto de Toledo[4]

[1]*Department of Nuclear Physics, Research School of Physical Sciences and Engineering, Australian National University, Canberra ACT 0200, Australia*

[2]*Yukawa Institute for Theoretical Physics, Kyoto University, Kyoto 606-8502, Japan*

[3]*Instituto de Física, Universidade Federal Fluminense, Av. Litoranea, Niterói, RJ, 24210-340, Brazil*

[4]*Instituto de Física, Universidade de Sao Paulo, Sao Paulo, S.P., Brazil*

(Received 7 August 2002; published 30 October 2002)

Excitation functions have been measured for the fusion of the weakly bound nuclei ^{6}Li and ^{7}Li with ^{209}Bi. The complete-fusion cross sections are lower than those predicted by fusion models, being only 65% and 75% for ^{6}Li and ^{7}Li, respectively. Within the uncertainties, this suppression is independent of beam energy. Distinguishing complete fusion from incomplete fusion, both experimentally and in theoretical models, is essential to understand the fusion process of weakly bound nuclei. A simple classical trajectory model which makes this distinction is presented. Further developments of the concepts of this model could be used for realistic predictions for the fusion of unstable weakly bound nuclei.

DOI: 10.1103/PhysRevC.66.041602 PACS number(s): 25.70.Jj, 25.70.Mn

Nuclei with extreme neutron/proton ratios may now be produced in fusion reactions with radioactive beams. For fusion to take place two nuclei must overcome the fusion barrier that results from the combination of the attractive nuclear and repulsive Coulomb potentials. The coupling between the relative motion and the intrinsic degrees of freedom of the participating nuclei leads at low energies to an enhancement [1,2] in fusion cross sections over predictions for a single fusion barrier. For unstable nuclei the fusion process can also be affected by their low binding energy, which can cause them to break up before reaching the fusion barrier. This may reduce the complete fusion cross sections, making it difficult to make nuclei with extreme neutron/proton ratios. It is therefore important to understand the effect of breakup of weakly bound nuclei on the fusion process.

Theoretically, the situation has been controversial [3–6]. Only recently has a qualitative model been proposed [7] which reconciles the conflicting approaches, predicting enhancement of fusion cross sections at sub-barrier energies, and a reduction at above-barrier energies. Fusion measurements with radioactive beams of ^{6}He [8,9], ^{11}Be [10,11], ^{17}F [12], and ^{38}S [13] do not show fusion suppression at above-barrier energies, and fusion with ^{6}He shows large enhancements at below-barrier energies, attributed to neutron transfer [8,9]. In contrast, measurements of the stable, but weakly bound ^{9}Be with ^{208}Pb showed [14] that above-barrier fusion cross sections are only 68% of those expected theoretically. Experimentally, reactions with weakly bound nuclei such as ^{6,7}Li and ^{9}Be are the best candidates to test theoretical models of breakup and fusion. Their breakup results in charged fragments which are easily detected and it is possible to separate the products of complete fusion and incomplete fusion, where only part of the projectile is captured. Reactions with ^{6}Li and ^{7}Li are simpler to model than those with ^{9}Be, as the former involve only a two-body breakup. The effect of different energy thresholds for breakup can be investigated by comparing ^{6}Li and ^{7}Li, which will also tie in with future measurements for ^{11}Li.

In this Rapid Communication we present precise fusion excitation functions for the ^{6}Li+ ^{209}Bi and ^{7}Li+ ^{209}Bi reactions, at energies spanning the fusion barrier. Comparison of these two systems allows, for the first time, a quantitative measurement of the effect of different breakup thresholds on fusion. Using ^{209}Bi as a target allows identification, through the decay α-particles, of complete-fusion products, where the whole projectile fuses with the target, as well as products of incomplete fusion/transfer.

The experiments were performed with pulsed ^{6,7}Li beams from the 14UD tandem accelerator at the Australian National University, incident on ^{nat}Bi targets 1 mg/cm^2 thick. The experimental conditions were similar to those reported in Ref. [14]. Aluminum catcher foils of thickness 180 μg/cm^2 placed immediately behind each target stopped the recoiling heavy reaction products. These were detected and identified by measuring the characteristic α-particle energies and lifetimes, ranging from 110 ns to 138 d, associated with their subsequent decay. Fission following fusion was measured during the irradiations, in two large area position sensitive multiwire proportional counters [14]. Absolute cross sections were determined by measuring sub-barrier elastic scattering in all detectors.

The compound nuclei ^{215}Rn and ^{216}Rn, formed following the fusion of ^{6}Li+ ^{209}Bi and ^{7}Li+ ^{209}Bi, respectively, are expected to cool mainly by neutron evaporation. The resulting Rn nuclei and their Po and At daughters were observed. However, the populations of Po and At nuclei were far in excess of those expected from Rn decay. In principle the excess could be due to αxn and $ypxn$ evaporation from the compound nucleus. This was ruled out, as no direct production of Po and At nuclei was found at a level of 0.5% of the xn products, when ^{216}Rn was formed at similar excitation energies following fusion of ^{18}O with ^{198}Pt. The excess Po and At yields are thus attributed to incomplete fusion and/or transfer, and are referred to as incomplete-fusion products. The cross sections for the Rn isotopes are shown in Figs. 1(a) and (b). Also shown are the measured fission cross sec-

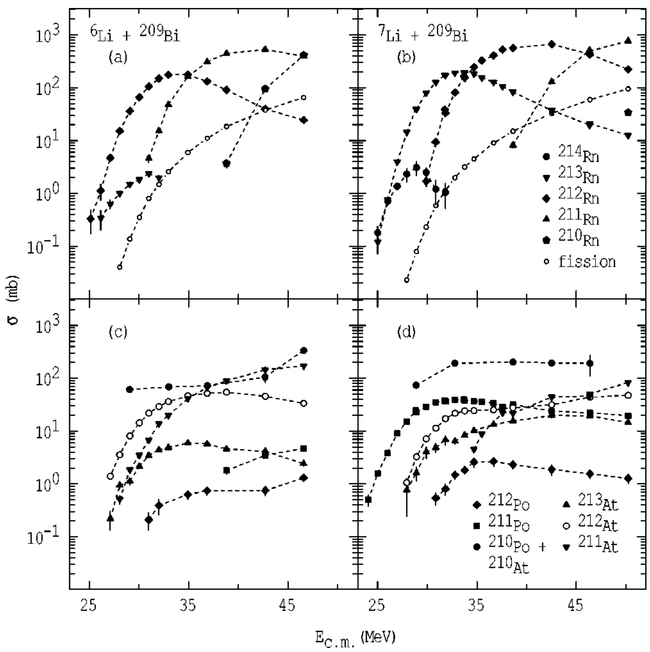

FIG. 1. Measured cross sections for fission and Rn isotopes for the two reactions (top panels). The bottom panels show the incomplete-fusion cross sections. The symbols denote the same products in the left and the right panels; the lines guide the eye.

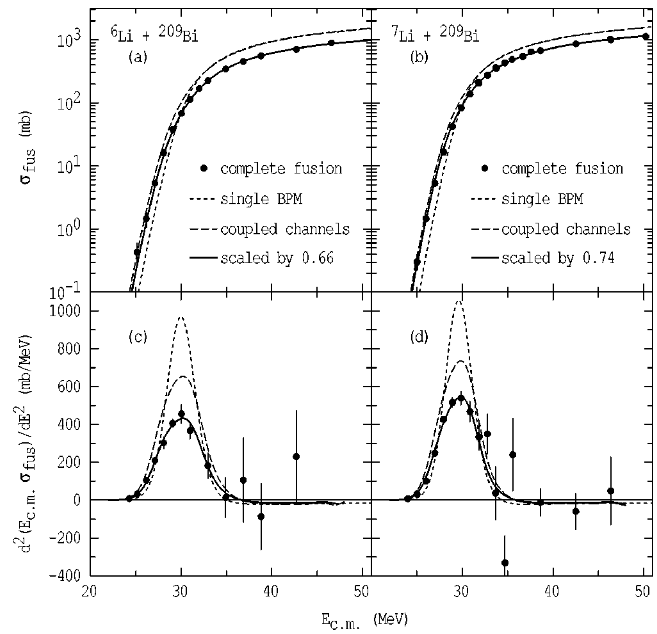

FIG. 2. The measured complete-fusion cross sections (top panels) and the experimental barrier distributions (bottom panels) for the reactions indicated. The short dashed lines result from single barrier penetration calculations, while the long dashed lines show the results of coupled-channels calculations. The full lines show the latter calculations scaled by factors indicated.

tions, attributed [14] to complete fusion. The cross sections for direct production of $^{210-212}$Po and $^{211-213}$At are shown in Figs. 1(c) and (d). The cross sections for ^{209}Po could not be determined due to its long half-life of 102 years. It can have a significant contribution for the ^{6}Li reaction at all energies, while its contribution for the ^{7}Li reaction should be significant only at the highest energies. The measured cross sections are in good agreement with those of Ref. [15], which however only cover a narrow energy range.

The cross section for complete fusion (σ_{fus}), defined experimentally as the capture of all the charge of the Li projectiles, was obtained by summing the Rn xn evaporation residue and fission cross sections at each energy. The results are shown in the upper panels of Fig. 2. From these, the experimental fusion barrier distributions shown in Figs. 2(c) and (d) were obtained [16] by taking the second derivative of the quantity $E_{\mathrm{c.m.}}\sigma_{\mathrm{fus}}$ with respect to the center-of-mass energy $E_{\mathrm{c.m.}}$ [17]. A step length of $\simeq 2$ MeV for energies $E_{\mathrm{c.m.}} \leqslant 37$ MeV and 3.5 MeV for higher energies was used. The average barrier energies were obtained by determining the centroids of these distributions [14], and are thus independent of suppression of the fusion cross sections. For ^{6}Li+ ^{209}Bi and ^{7}Li+ ^{209}Bi the barriers are 30.1 ± 0.3 MeV and 29.7 ± 0.2 MeV, respectively; the predictions using the Woods-Saxon form of the Akyüz-Winther [18] nuclear potential are 30.40 MeV and 30.04 MeV, respectively.

To determine the above-barrier fusion suppression, the data were compared with the predictions of a single barrier penetration model (SBPM) and a coupled channels code [19]. A Woods-Saxon nuclear potential with diffuseness of 0.63 fm and depth adjusted to reproduce the measured average barrier energies was used. Predictions of the complete-fusion cross sections and barrier distribution using a coupled channels model require a good understanding of the couplings to unbound states and their effect on fusion. Since this has not yet been achieved, couplings were chosen only to reproduce the shape of the measured barrier distributions, in order to demonstrate that fusion suppression above the barrier is insensitive to the couplings (as long as the average barrier position from the calculations matches that of the experiment). The results of the single barrier penetration model (short-dashed lines) and coupled channels (long dashed lines) calculations are compared with the data in Fig. 2. As expected, at energies below the average barrier the measured cross sections for both reactions are larger than the predictions of the SBPM by a factor of $\simeq 5$. At above-barrier energies the SBPM calculations and the coupled channels calculations are in close agreement, as expected. However, the measured cross sections lie below these predictions. Using the data above $E_{\mathrm{c.m.}} = 36$ MeV, for ^{6}Li and ^{7}Li they are, respectively, 65^{+6}_{-5}% and 73^{+6}_{-4}% of the SBPM predictions, and 66^{+6}_{-5}% and 74^{+6}_{-4}% of the coupled channels cross sections. The uncertainties arise mainly from uncertainties in the average barrier energies, and the effect of varying the diffuseness of the nuclear potential by ± 0.2 fm. These uncertainties do not affect the relative suppression of ^{6}Li to ^{7}Li, which is much better defined, and is determined to be 0.89 ± 0.02. The suppression of fusion can also be determined by comparing the measured and calculated areas under the barrier distributions. The suppression determined using this method is independent of the exact nature of the couplings, since inclusion of couplings changes the shape of the barrier distribution but preserves the area under it. Using the cross sections for $E_{\mathrm{c.m.}}<36$ MeV, the area for ^{6}Li is 64^{+5}_{-4}% and for ^{7}Li is 76^{+5}_{-4}% of the model predictions. The uncertainties arise mainly due to the ±0.2 fm range assigned to the diffuseness of the nuclear potential. Thus the fusion suppression factor appears to be independent of beam energy.

The reduction in complete fusion is interpreted as arising from breakup of the projectile into an α particle and a deuteron (for ^{6}Li) or triton (for ^{7}Li). The probability of breakup is expected to be determined by the breakup Q values and the coupling strengths to unbound states. The larger reduction in above-barrier cross sections for ^{6}Li is correlated with its lower breakup threshold of 1.47 MeV compared with 2.47 MeV for ^{7}Li.

The ^{6,7}Li$+^{209}$Bi, as well as the ^{9}Be$+^{208}$Pb [14] reactions, clearly show that the complete-fusion cross sections at energies above the barrier are suppressed compared to expectations for the fusion of tightly bound nuclei. However, for all three reactions, the sum of complete- and incomplete-fusion cross sections at energies above the barrier matches [14] or slightly exceeds the calculated fusion cross sections. Thus, if experimentally the complete- and incomplete-fusion products are not identified separately but instead are summed, then no suppression of fusion will be apparent.

Understanding the effect of breakup on fusion requires modelling of the complete dynamics, including (i) couplings to bound and continuum states, (ii) an appropriate co-ordinate system to describe the physical boundary condition for the wave functions of the breakup fragments, and (iii) modelling of the trajectories of the breakup fragments to determine whether one or both fragments are captured by the target nucleus. Most theoretical models [20–23] describing reactions of weakly bound nuclei are only appropriate for calculating elastic scattering and transfer/breakup cross sections, as (ii) and (iii) are not included in these models. A recent calculation [7] has attempted to address this issue by identifying absorption from the projectile bound states as complete fusion, and that from the unbound states as incomplete fusion. Although this calculation has qualitatively explained the observations, it provides only an upper limit to the suppression, since the possibility that following breakup, all the fragments could subsequently fuse with the target is not accounted for. In contrast with this physical approach, it has recently been claimed [24] that a similar suppression of fusion can be generated by coupling to excited states within a simplified coupled-channels model. These calculations did not incorporate any of the properties of unbound nuclei, the spurious suppressions resulting from using an unphysically large coupling strength together with an unphysically small breakup Q value.

In order to follow the path of the breakup fragments, we have developed a three-body classical trajectory model. For the Hamiltonian of a three-particle system that consists of the target (T) and two projectile fragments ($P1$ and $P2$), two-dimensional classical Newtonian equations are solved to obtain the time evolution of the co-ordinates and velocities of the fragments. The initial conditions are that the projectile, with its two fragments in random orientation, starts far from the target with impact parameter b. As the projectile moves towards the target, the interactions between the target and

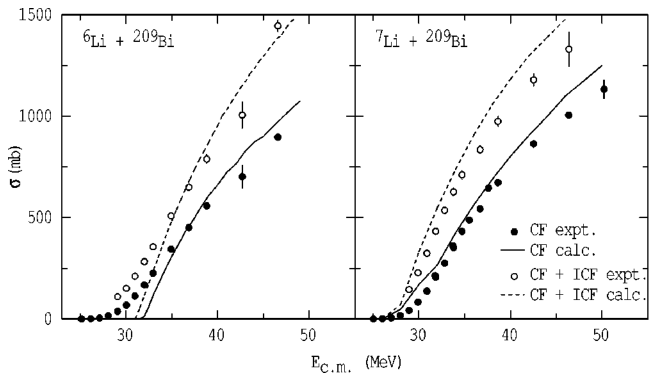

FIG. 3. The measured and calculated complete-fusion (CF) and the sum of complete- and incomplete-fusion (ICF) cross sections for (a) ^{6}Li$+^{209}$Bi, and (b) ^{7}Li$+^{209}$Bi reactions. The calculations are from the three-body classical trajectory model (see text).

projectile fragments cause potential and kinetic energy to be converted to relative kinetic energy between the two fragments. Breakup of the projectile occurs when the relative kinetic energy and relative distance between $P1$ and $P2$ exceed their potential barrier height and barrier radius, respectively. The potential between $P1$ and $P2$ is assumed to be given by $V_{12}(r)=Q_{BU}$ for $r<r_0$ and $V_{12}(r)=V_{12}^N(r)+V_{12}^C(r)$ for $r\geqslant r_0$, where V_{12}^N and V_{12}^C are, respectively, the nuclear and Coulomb potentials between $P1$ and $P2$, Q_{BU} is the Q value of the breakup process, and r_0 is the smallest distance which satisfies $V_{12}^N(r_0)+V_{12}^C(r_0)=Q_{BU}$. The Woods-Saxon form of the Akyüz-Winther potential is used for the nuclear potentials between the three particles. When the distance between the target and the projectile fragment Pi is smaller than $r_{\mathrm{abs}}=1.1\times(A_T^{1/3}+A_{Pi}^{1/3})$ fm, we assume that the fragment is absorbed by the target nucleus. Three processes are possible, depending on the value of the impact parameter b: (i) the projectile as a whole or both of the fragments are absorbed by the target, (ii) only one fragment is absorbed, and (iii) neither fragment is captured. These processes are associated with complete fusion, incomplete fusion, and breakup/scattering, respectively. The model calculations show that the projectile breakup occurs close to the fusion barrier radius, in agreement with recent experimental observations for the breakup of ^{9}Be [25]. This can result in a large probability of both fragments being captured by the target.

The calculated cross sections for complete fusion (full lines) and the sum of complete and incomplete fusion (dashed lines) are shown in Fig. 3, along with the measured quantities. The simple classical model is able to qualitatively describe the experimental data. The complete-fusion cross sections have two contributions, the first where the projectile fuses as a whole, and the second where both the fragments (following breakup) are captured by the target. Significantly, the model shows that at energies 10% above the fusion barrier, more than one-third of the complete fusion results from breakup followed by capture of both fragments. This contribution decreases with increasing energy. Complete fusion following breakup has previously been neglected in model calculations [7,26], and the present calculations show for the first time its importance. The predicted fusion suppressions are larger for ^{6}Li than ^{7}Li at the highest energies. However, quantitative agreement with the experimetally observed suppression is not obtained. Calculation of breakup probabilities from continuum discretized coupled channels calculations, followed by classical modelling of fragment trajectories, would give a more realistic picture of the interplay between breakup and fusion.

In summary, the complete-fusion cross sections for ^{6}Li, ^{7}Li+ ^{209}Bi show suppressions of 65% and 75%, respectively, within uncertainty being independent of beam energy. The suppression is attributed to breakup of the weakly bound projectiles. The larger suppression for ^{6}Li is correlated with the lower breakup threshold, and will provide a quantitative test of future realistic models of breakup and fusion. We have taken an important step in this direction through a simple classical trajectory model, which shows that at energies close to the fusion barrier, a large fraction of the complete fusion can be due to capture of both breakup fragments, a process which has been ignored in all previous models. A more sophisticated model, incorporating quantum mechanical couplings and classical fragment trajectories is planned, which should lead to a quantitative understanding of fusion involving weakly bound systems.

The work of M.D. was supported by the Australian Research Council. The work of S.B.M., P.R.S.G., R.M.A., N.C., and A.S.T. received partial support from CNPq, CAPES, FAPESP, and FAPERJ.

[1] C.H. Dasso *et al.*, Nucl. Phys. **A405**, 381 (1983).
[2] M. Dasgupta *et al.*, Annu. Rev. Nucl. Part. Sci. **48**, 401 (1998), and references therein.
[3] M.S. Hussein *et al.*, Phys. Rev. C **46**, 377 (1992); Phys. Rev. Lett. **72**, 2693 (1994); Nucl. Phys. **A588**, 85c (1995).
[4] N. Takigawa, *et al.*, Phys. Rev. C **47**, R2470 (1993).
[5] C.H. Dasso *et al.*, Phys. Rev. C **50**, R12 (1994); Nucl. Phys. **A597**, 473 (1996).
[6] K. Yabana, Prog. Theor. Phys. **97**, 437 (1997).
[7] K. Hagino *et al.*, Phys. Rev. C **61**, 037602 (2000).
[8] J.J. Kolata *et al.*, Phys. Rev. Lett. **81**, 4580 (1998).
[9] M. Trotta *et al.*, Phys. Rev. Lett. **84**, 2342 (2000).
[10] A. Yoshida *et al.*, Phys. Lett. B **389**, 457 (1996).
[11] C. Signorini *et al.*, Eur. Phys. J. A **2**, 227 (1998).
[12] K.E. Rehm *et al.*, Phys. Rev. Lett. **81**, 3341 (1998).
[13] K.E. Zyromski *et al.*, Phys. Rev. C **55**, R562 (1997).
[14] M. Dasgupta *et al.*, Phys. Rev. Lett. **82**, 1395 (1999).
[15] H. Freiesleben *et al.*, Phys. Rev. C **10**, 245 (1974).
[16] J.R. Leigh *et al.*, Phys. Rev. C **52**, 3151 (1995).
[17] N. Rowley *et al.*, Phys. Lett. B **254**, 25 (1991).
[18] R. A. Broglia and A. Winther, *Heavy Ion Reactions*, Vol. 1 (Benjamin/Cummings, Reading, MA, 1981).
[19] K. Hagino *et al.*, Comput. Phys. Commun. **123**, 143 (1999).
[20] Y. Sakuragi *et al.*, Prog. Theor. Phys. Suppl. **89**, 136 (1986)
[21] Y. Hirabayashi *et al.*, Phys. Lett. B **221**, 227 (1989).
[22] N. Keeley and K. Rusek, Phys. Lett. B **427**, 1 (1998).
[23] J.A. Tostevin *et al.*, Phys. Rev. C **63**, 024617 (2001).
[24] V. Tripathi *et al.*, Phys. Rev. Lett. **88**, 172701 (2002).
[25] D. J. Hinde *et al.*, Phys. Rev. Lett. (submitted).
[26] A. Diaz-Torres *et al.*, Phys. Rev. C **65**, 024606 (2002).